

Predictive path following based on adaptive line-of-sight for underactuated autonomous surface vessels

Liu, Chenguang; Negenborn, Rudy R.; Chu, Xiumin; Zheng, Huarong

DOI

[10.1007/s00773-017-0486-2](https://doi.org/10.1007/s00773-017-0486-2)

Publication date

2018

Document Version

Final published version

Published in

Journal of Marine Science and Technology

Citation (APA)

Liu, C., Negenborn, R. R., Chu, X., & Zheng, H. (2018). Predictive path following based on adaptive line-of-sight for underactuated autonomous surface vessels. *Journal of Marine Science and Technology*, 23(3), 483-494. <https://doi.org/10.1007/s00773-017-0486-2>

Important note

To cite this publication, please use the final published version (if applicable). Please check the document version above.

Copyright

Other than for strictly personal use, it is not permitted to download, forward or distribute the text or part of it, without the consent of the author(s) and/or copyright holder(s), unless the work is under an open content license such as Creative Commons.

Takedown policy

Please contact us and provide details if you believe this document breaches copyrights. We will remove access to the work immediately and investigate your claim.

Predictive path following based on adaptive line-of-sight for underactuated autonomous surface vessels

Chenguang Liu^{1,2}  · Rudy R. Negenborn² · Xiumin Chu¹ · Huarong Zheng²

Received: 6 December 2016 / Accepted: 3 October 2017 / Published online: 24 October 2017
© JASNAOE 2017

Abstract Underactuated autonomous surface vehicles (ASVs) have stringent requirements on automatically tracking a predefined path. This paper proposes a model predictive control (MPC) approach based on adaptive line-of-sight (LOS) guidance for path following of ASVs. For the controller, a second-order nonlinear Nomoto model with disturbances is proposed as the vessel dynamic motion model after reviewing and comparing different ship motion models applied for path following control. For the guidance system, a novel adaptive LOS guidance with a variable acceptance circle radius is proposed to improve the precision of reference path tracking. Specifically, the acceptance circle radius is adapted with the angle between two adjacent straight segments of a reference path. Simulation experiments illustrate that the LOS guidance system with a variable acceptance circle radius results in smaller tracking errors compared with the fixed acceptance circle radius. The proposed path following method can track reference paths well even in the face of disturbances.

Keywords Path following · Model predictive control · Line-of-sight · Nomoto model · Autonomous surface vessels

1 Introduction

The use of autonomous surface vehicles (ASVs) for both military and civil applications has been growing fast in recent years [1]. As an important part of autonomy or automatic collision avoidance for ASVs, path following has received much attention in the academic field [2–4]. One challenge of path following for a surface vessel stems from the fact that vessels are often underactuated without an actuator in the sway axis [5]. Therefore, the transverse speed and acceleration for an underactuated vessel can be adjusted only by a rudder and a longitude propeller. This can lead to difficulties in reducing cross-tracking errors (the vertical distance between the vessel and the reference path) in path following. To achieve better performance of path following, complex vessel motion models have been used in [6]. However, to apply path following methods based on those models in practice, many parameters of the models need to be identified. Meanwhile, the precision of model parameters can hardly be guaranteed as those parameters may be time varying.

For path following, Fossen [7] proposed a systematic design involving three subsystems, namely, guidance, navigation, and control. Specifically, the guidance subsystem is used for guiding the path of a marine craft; the navigation subsystem is used for determination of the position, attitude, speed, heading, etc.; and the control subsystem is used for motion control. Adapted from [7], we propose the architecture of a path following system for underactuated ASVs, as presented in Fig. 1. In this architecture, we assume that the navigation subsystem as the perception system is available, and the guidance and control subsystem combined together into the decision system. The guidance subsystem consists of a path generator and the line-of-sight (LOS) guidance algorithm; the control subsystem is implemented by model

✉ Chenguang Liu
liuchenguang@whut.edu.cn

¹ National Engineering Research Center for Water Transport Safety, Wuhan University of Technology, Wuhan 430063, People's Republic of China

² Department of Maritime and Transport Technology, Delft University of Technology, 2628 CD Delft, The Netherlands

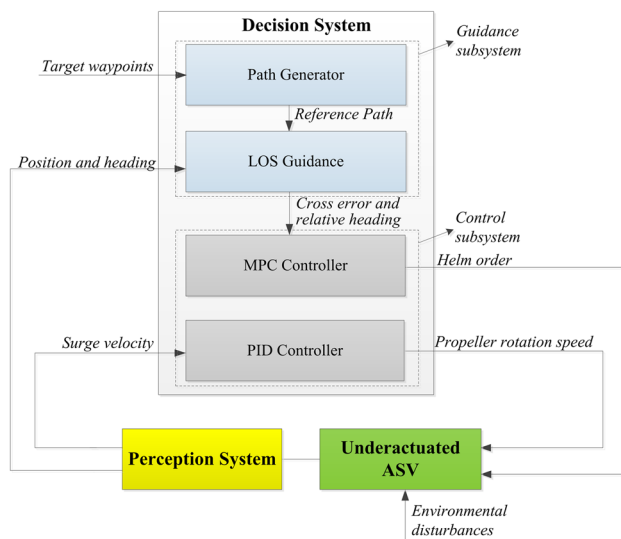


Fig. 1 Path following control architecture

predictive control (MPC) and proportional–integral–derivative (PID) controllers. System inputs, namely, ship propeller speed and rudder angle, can be calculated with this decision system given target waypoints and vessel states. In this paper, we focus on the decision system and discuss how to design a controller to improve the accuracy of path following. PID controller design is not discussed in this paper, since PID controller is mature enough.

Given target waypoints, the reference path is generated either as a sequence of straight lines or as a sequence of curve segments [7]. For path following problems, the former is usually adopted. When the reference path has been generated, the next problem is to determine how to track the path precisely in an energy-efficient way. The most popular approach is to simplify the tracking problem as a regulation problem by adopting path following error dynamics [5]. The LOS guidance approach is widely used for calculating the tracking heading that reduces the cross-tracking error fast. A conventional autopilot is realized using LOS guidance with PID-based heading controller in [8]. LOS guidance is not only used to extend the straight-line path following to arbitrary path following, but also used to give more natural motions in the longitudinal direction by the use of rudder as in [9, 10]. Some pioneering work was carried out by McGookin et al. [11] and Fossen et al. [12] who applied the LOS guidance to path following problems of surface vessels, and by Wilson et al. [13] who introduced the LOS guidance to aid manoeuvre decision making for collision avoidance based on a two-ship encounter. Later, Moreira et al. [6] used a variable LOS circle radius, so that an intersection between the LOS circle and the path always exists. Oh et al. [8] used a variable lookahead distance to obtain higher tracking accuracy. When the reference heading has been obtained by LOS,

the vessel heading should be adjusted to the LOS reference heading by controlling the rudder angle to track the reference path.

Related control methods, for instance, PID, backstepping, sliding mode control, and MPC, were proposed and applied in controlling ship motion in recent years [8, 14, 15]. The conventional tracking control systems for surface vehicles are usually implemented using a standard PID autopilot together with LOS guidance [8]. For path following problems of underactuated vessels that only have two degrees of freedom, it is more difficult to control the vessel trajectory because of the lack of sway freedom. The manoeuvrability difference between an underactuated and a fully actuated vessel causes that underactuated vessels typically need more time to converge to the path. Moreover, rudder magnitude and rate constraints should be taken into consideration to avoid failure of actuators [8]. MPC offers a good choice to handle these challenges at the same time because of its advantage of considering constraints explicitly. An MPC controller for the integrated path following and roll motion control problem was proposed by Liu et al. [9]. The predictive path following with MPC considering time and logic constraints was reported by Zheng et al. [16].

MPC methods rely on system models for predictions. On the one hand, the model should be precise enough to describe the motion of a vessel. On the other hand, the model should have parameters that are easy to identify. The most widely used ship model in path following research is the hydrodynamic model developed by Fossen [5]. In this model, the ship's inertial and damping parameters need to be identified. These parameters can be obtained by a series of hydrodynamic tests in a towing basin. However, it is generally difficult to conduct such tests when considering a full ship size. Moreover, some of the parameters can always vary, because ship draught and gravity centres change during sailing. A conventional autopilot has been widely used with the first-order Nomoto model [17]. Nomoto models are derived from hydrodynamic models, whose parameters are easier to identify with a turning or a zigzag pattern test in open water. Compared with the first-order linear Nomoto model, the second-order nonlinear Nomoto model can take into account nonlinear terms, e.g., surge-sway motion couplings. To the best of our knowledge, the second-order nonlinear Nomoto model has not been applied for path following before.

This paper proposes a path following algorithm based on LOS guidance and MPC. For the LOS guidance, a novel adaptive LOS method with variable acceptance circle radii is proposed. The relationship between the acceptance circle radius and the angle between two adjacent straight segments of a reference path is deduced. We carry out several simulation experiments to illustrate the necessity and effectiveness of the proposed adaptive LOS method. Considering the feasibility of identifying parameters of hydrodynamic

models as well as the accuracy of modeling vessel motions, the second-order nonlinear Nomoto model is used for controller design. Based on the model, an MPC controller is designed to control the vessel to track the predefined path satisfying system constraints. Simulation experiments without and with disturbances illustrate the effectiveness of the proposed algorithm.

The remainder of this article is organized as follows. The surface vessel models used for path following are reviewed in Sect. 2. In Sect. 3, the conventional LOS guidance is presented first, the LOS algorithm with adaptive acceptance circle radius is proposed subsequently, and the Nomoto-based MPC-based controller is derived at last. In Sect. 4, simulation experiments are carried out to verify the performance of the controller. Conclusions and future work directions are presented in Sect. 5.

2 Surface vessel models

Many kinds of surface vessel models have been used in path following in different applications. Kinematics and kinetics models from one to six DOFs with environmental disturbance forces and moments have been derived and elaborated in [7]. These models can be used in applications such as course keeping, dynamic positioning, trajectory tracking, and path following. In this section, we focus on models that can be used for path following. The inertial motion coordinate is defined as $\{n\} = \{x_n, y_n\}$, and the body-fixed coordinate system is defined as $\{b\} = \{x_b, y_b\}$, as shown in Fig. 2, where U and ϕ are the velocity and course in $\{n\}$, respectively; ψ and r stand for the vessel heading angle and yaw rate in system $\{n\}$, respectively; δ (τ_r) and n (τ_u) stand for rudder angle (rudder torque) and propeller rotation speed (thrust force), respectively. Note that the heading angle ψ is different from the vessel course γ and $\gamma = \beta + \psi$. The drift angle β is equal to 0 only when the sway velocity $v = 0$ and

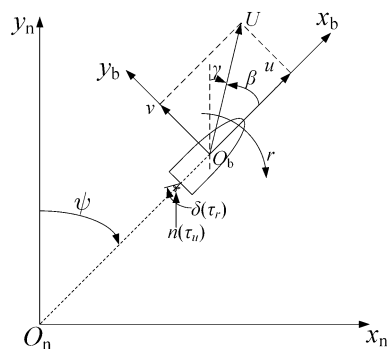


Fig. 2 Motion coordinate systems for an underactuated surface vessel. Adapted from [18]

there is no current. A 6 DOF model for an surface vessel can be denoted as follows [7]:

$$\tau + \tau_{wind} + \tau_{wave} = M_{RB} \dot{v} + M_A \dot{v}_r + C_{RB}(v)v + C_A(v_r)v_r + D(v_r)v_r + g(\eta) + g_0, \quad (1)$$

where $v = [u, v, w, p, q, r]^T$ is the velocity vector of surge, sway, heave, roll, pitch, and yaw in $\{b\}$; $v_r = [u_r, v_r, w_r, p_r, q_r, r_r]^T$ is the relative velocity vector between ship hull and the fluid; $\eta = [x, y, z, \phi, \theta, \psi]^T$ is the position/Euler angles; the model matrices M_{RB} and M_A , $C_{RB}(v)$ and $C_A(v)$, and $D(v)$ denote inertia, Coriolis, and damping, respectively; τ is the system input vector of forces and moments; τ_{wind} and τ_{wave} are the vectors of forces and moments generated by wind and wave, respectively; $g(\eta)$ is the vector of gravitational and buoyancy forces; and g_0 is the static restoring forces and moments. We classify these models into different categories by four criterion and propose the most suitable model for path following controller design in this paper.

2.1 Category of models for path following

We categorize different surface vessel models for path following as linear and nonlinear models, models with disturbances and without disturbances, and models with different DOFs and models with different input types, as shown in Table 1.

2.1.1 Linear or nonlinear models

Linear models In controller design, linear models have the advantages of being simple and being computationally efficient in cases, where real-time calculations are required. It is proposed that a linear model is used for controller design and a nonlinear model for simulation [19]. [6, 9, 20, 21] use linear models for path following derived from (1) by assuming the surge speed constant, so that the surge dynamics are neglected.

Nonlinear models However, motions of surface vessels always have nonlinear characteristics due to nonlinear Coriolis, centripetal forces, damping, etc. [7]. Incorporating the nonlinear terms in (1) makes the modeling of vessel behaviors more accurate especially when assumptions underlying the linear models are not satisfied. In those nonlinear models in Table 1, the surge velocity u is variable.

2.1.2 Models without disturbances or with disturbances

Models without disturbances Disturbances usually include environmental disturbances and system uncertainties during path following. When there are no disturbances existing or when they are ignored for the sake of simplicity, a path

Table 1 Different models used for path following

Literature	Nonlinear	Linear	Without disturbances	With disturbances	Surge, sway, yaw	Surge, sway, yaw, roll	Sway, yaw	Surge force, sway force, yaw moment	Surge force, yaw moment	Surge force, rudder angle	Rudder angle	Yaw moment
[16, 20, 23, 32]	•			•	•			•				
[2, 14, 26, 27, 29, 33, 34]	•			•	•			•				
[5, 12, 35]	•		•	•	•			•				
[22, 24]	•			•	•							
[8, 30]	•		•	•	•							
[28]	•			•	•							
[36]	•			•	•							•
[9]		•		•	•						•	
[20]		•		•	•						•	
[6]		•		•	•						•	
[21]		•		•	•		•					•

following controller can be designed without considering disturbances, as done in [5, 6, 9, 12]. For (1), the disturbances are neglected with $v_r = v$, $\tau_{wind} = 0$ and $\tau_{wave} = 0$.

Models with disturbances Disturbances are prevalent and have various influences on control performance. For instance, nonvanishing disturbances may destroy the stability of a control system [2]. Therefore, it is essential to take into account disturbances in controller design of path following. In (1), the disturbances consist of current, wind, and wave forces and moments. However, models in [16, 22–24] only consider disturbances with current velocity v_c which is usually assumed as irrotational and constant.

2.1.3 Models with different DOFs

A vessel that can move freely in the 3D space has a maximum of 6 DOFs (surge, sway, heave, roll, pitch, and yaw), three translational and three rotational components [7]. The 6 DOF model is seldom used for controller design because of their complexity. In fact, some DOFs can be neglected during path following of surface vessels. The most popular models have 3 DOFs in the horizontal plane, i.e., surge, sway, and yaw [25–27]. To simplify the model, the surge speed can be kept constant and a 2 DOFs model is obtained, i.e., only considering sway and yaw [6]. For some circumstances, it is necessary to add the roll DOF into the 3 DOF model to set a roll constraint to improve safety and comfort [9, 20, 28]. Neglecting no roll, pitch or heave DOF in (1), both $g(\eta)$ and g_0 can be assumed as 0.

2.1.4 Models with different input types

There are several types of model inputs with different levels of modeling details, i.e., forces and moments, or rudder angle and propeller rotation speed with modeling of even lower lever actuator dynamics. In [16, 26, 29], the system inputs are forces and moments that are generated by the actuators, i.e., propeller and rudder. When the inputs are generated by these models, it is necessary to handle the controller allocation problem, i.e., distributing the generalized control forces and moments to the actuators in terms of control inputs, such as rudder angle and propeller rotation speed [7]. However, in [9, 20, 30], the model input is only the rudder angle, which means that the controller allocation is completed with the model.

2.1.5 Summary

Models that involve nonlinear terms, disturbances terms, and more DOFs will be more accurate theoretically. However, models with these features lead to more computational burden. At the same time, more complicated models imply more identification difficulties. Usually, parameter identification

of some models is complicated even with the help of towing carriage in a tank [31]. The towing carriage can serve for resistance and propulsion tests which are used to identify the various parameters of models. Parameter identification experiments are hardly completed with real vessel due to the towing tank size and expensive considerations. If we use a model ship to substitute the corresponding real vessel for parameter identification, the identified values of parameter are not always fully consistent with the real ones, because the differences between a real vessel and a model one always exist. Moreover, if inputs of a model are forces and moments, the model can be used in practice only when the inputs are transformed into propeller rotation speed and rudder angle. Therefore, we should consider them synthetically when choosing a model for path following. Most surface vessel models in Table 1 have been used only in numerical simulations because of the challenges of identifying of parameters as well as the time-varying nature of those parameters.

2.2 Proposed model

In path following, the sway speed for an underactuated vessel always stays small and the surge speed can be deemed as constant [5, 6, 8]. In this paper, to avoid challenges in parameter identification while taking into account nonlinear characteristics of ship dynamics, we propose to use the Nomoto second-order nonlinear model as the vessel motion dynamic model which is as follows:

$$T_1 T_2 \ddot{\psi} + (T_1 + T_2) \dot{\psi} + \psi + \alpha \psi^3 = K(\delta + T_3 \dot{\delta}), \tag{2}$$

where ψ is the heading and $\dot{\psi} = r$ in which r is the angular velocity of yaw; δ is the rudder angle; K is the Nomoto gain; T_1, T_2 , and T_3 are manoeuvrability indices; and α is a nonlinear coefficient. To use model (2), parameters T_1, T_2, T_3, K , and α should be identified.

Compared with other models that do not pertain to Nomoto ones, model (2) only has one input, namely, the rudder angle, and one output, namely the heading. The involved two parameters, i.e., rudder angle δ and heading ψ , can be obtained easily and precisely with angular transducer gyrocompass, respectively. However, models involving speed data that is hard obtained because of difficulties of high positioning accuracy.

The rudder of a vessel is usually driven by a steering engine. Characteristics of the rudder servo system are modelled by [37]:

$$T_C \dot{\delta} + \delta = K_C \delta_C, \tag{3}$$

where δ_C is the helm order controlled by a course controller, δ is the actual rudder angle, K_C is the rudder gain, and T_C is the rudder time constant.

Here, we propose a model that combines (2) and (3) for the path following of ASVs. When setting system states and input as $\mathbf{x} = [x_1 \ x_2 \ x_3 \ x_4]^T = [\psi \ r \ \dot{\delta}]^T$ and $u = \delta_C$, respectively, we transform (2) and (3) into the following state-space form:

$$\dot{\mathbf{x}} = f(\mathbf{x}, u) = \begin{bmatrix} x_2 \\ x_3 \\ g_1(\mathbf{x}, u) \\ \frac{1}{T_C}(K_C u - x_4) \end{bmatrix}, \tag{4}$$

where $g_1(\mathbf{x}, u)$ can be denoted by

$$g_1(\mathbf{x}, u) = \frac{1}{T_1 T_2} [Kx_4 + \frac{KT_3}{T_C}(K_C u - x_4) - (T_1 + T_2)x_3 - x_2 - \alpha x_2^3].$$

Due to the presence of disturbances, model (4) is rewritten as follows:

$$\dot{\mathbf{x}}(t) = f(\mathbf{x}(t), u(t)) + \mathbf{E}\mathbf{w}(t), \tag{5}$$

where $\mathbf{E} \in \mathbb{R}^{4 \times 4}$ is the disturbance input matrix, and $\mathbf{w}(t) \in \mathbb{R}^{4 \times 1}$ is an unknown but bounded random disturbance vector. The proposed model (5) can be categorized according to Table 1 as a nonlinear model with disturbances of which the input and one DOF is the rudder angle and yaw, respectively.

3 Decision system design

In this section, we will design the two key components of the decision system in Fig. 1: the adaptive LOS guidance algorithm and the nonlinear MPC controller based on model (5).

3.1 Adaptive LOS guidance

3.1.1 Traditional LOS guidance

A typical reference path, as shown in Fig. 3, can be considered as several straight line segments generated by connecting waypoints $P_n(x_n, y_n), P_{n+1}(x_{n+1}, y_{n+1}), P_{n+2}(x_{n+2}, y_{n+2})$, etc. The ship actual position is $O_b(x_b, y_b)$.

In LOS guidance, an underactuated vessel controlled only with a rudder tracks the reference path based on the difference between the heading angle ψ and the LOS angle ψ_{LOS} that can be calculated with a LOS point $P_{LOS}(x_{LOS}, y_{LOS})$. There are three ways to generate the LOS points on the path:

1. to set the waypoint P_{n+1} as the LOS point P_{LOS} [9];

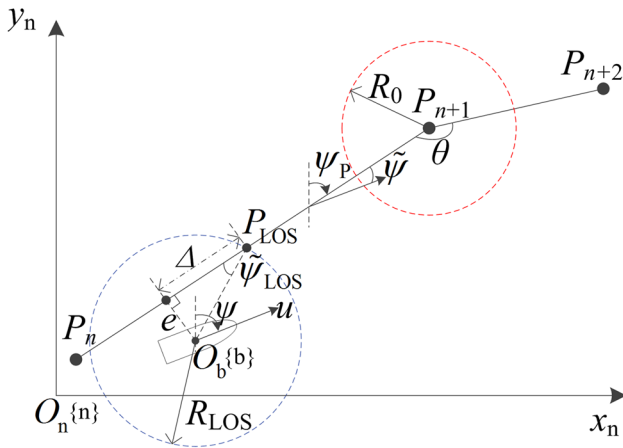


Fig. 3 LOS guidance for path following

2. based on the cross-tracking error e and a lookahead distance $\Delta = nL$ (n denotes positive integer and L denotes the ship length) [8];
3. based on e and a circle of radius $R_{LOS} = nL$ around O_b [6].

The first approach results in large cross errors in the presence of environmental disturbances. The second approach may increase difficulties in converging to the path when there exist large cross errors. Therefore, the third approach is employed in this paper as in [6]. The LOS point P_{LOS} is calculated by solving the following equations [12]:

$$(x_{LOS} - x_b)^2 + (y_{LOS} - y_b)^2 = R_{LOS}^2, \tag{6}$$

$$\frac{y_{LOS} - y_n}{x_{LOS} - x_n} = \frac{y_{n+1} - y_n}{x_{n+1} - x_n}. \tag{7}$$

Two solutions corresponding to the two intersections between the circle and the path can be obtained by solving the above equations. The closer intersection to the current waypoint, i.e., P_{n+1} in Fig. 3, is selected as P_{LOS} .

The transformation for the body-fixed velocities to the inertial velocities is as follows:

$$\begin{cases} \dot{x}_b = u \sin \psi - v \cos \psi \\ \dot{y}_b = u \cos \psi + v \sin \psi \end{cases} \tag{8}$$

Define the ship heading relative to the path as $\tilde{\psi} = \psi - \psi_P$, where ψ_P is the path direction. Then, differential equations of e and $\tilde{\psi}$ can be denoted by [38]:

$$\dot{e} = u \sin \tilde{\psi} + v \cos \tilde{\psi}, \tag{9}$$

$$\dot{\tilde{\psi}} = r. \tag{10}$$

In (9), e is the cross-tracking error, i.e., the vertical distance from O_b to the objective path $P_n P_{n+1}$. The surge speed u is assumed to be constant as u_0 ($u_0 > 0$), and the sway speed v

is generally small and thus assumed as $v \approx 0$ [5, 6]. Therefore, (9) is simplified as

$$\dot{e} = u_0 \sin \tilde{\psi}, \tag{11}$$

Based on e and R_{LOS} , the LOS angle $\tilde{\psi}_{LOS}$ is denoted as

$$\tilde{\psi}_{LOS} = -\arcsin\left(\frac{e}{R_{LOS}}\right), \tag{12}$$

where $\tilde{\psi}_{LOS} \in [-\frac{\pi}{2}, \frac{\pi}{2}]$. To track the path $P_n P_{n+1}$, we make the angle $\tilde{\psi}$ satisfy $\tilde{\psi} \rightarrow \tilde{\psi}_{LOS}$. Then, we have

$$\dot{e} = u_0 \sin \tilde{\psi}_{LOS} = -\frac{u_0}{R_{LOS}} e. \tag{13}$$

To demonstrate e converge to 0, we use the Lyapunov’s second method. We know that $e = 0$ is an equilibrium point of (13). The Lyapunov function is set as $V(e) = e^2$, and we have

$$\dot{V}(e) = 2e\dot{e} = -\frac{u_0}{R_{LOS}} e^2 \leq 0 (u_0 > 0), \tag{14}$$

where $\dot{V}(e) = 0$ only when $e = 0$. Therefore, (13) has global asymptotic stability, i.e., $e \rightarrow 0$ globally as $\tilde{\psi} \rightarrow \tilde{\psi}_{LOS}$.

To guarantee that there is always a real solution to (12), the LOS circle radius is set as

$$R_{LOS} = \begin{cases} 3L, & \text{for } e \leq 3L \\ e + L, & \text{otherwise.} \end{cases} \tag{15}$$

Switching to the next waypoint P_{n+2} relies on whether the vessel is within an acceptance circle around the current waypoint P_{n+1} or not. If the vessel position O_b satisfies $(x_b - x_{n+1})^2 + (y_b - y_{n+1})^2 \leq R_0^2$, the waypoint will be changed to P_{n+2} . To guarantee that the solutions to (6) always exist, we need $R_{LOS} \geq R_0$. The acceptance circle radius R_0 is usually set as a constant based on ship length, for instance, L or $2L$ [6]. However, the value of R_0 has an influence on the performance of path following that has been compared briefly in [6] without further analysis and solutions. In the next subsection, we propose an adaptive acceptance circle radius method to improve the performance of path following.

3.1.2 Adaptive LOS guidance with variable acceptance circle radius

When the vessel is within the acceptance circle, it inevitably deviates from the predefined path because both the LOS angle $\tilde{\psi}_{LOS}$ and relative heading angle $\tilde{\psi}$ change suddenly. If the radius R_0 is too small with small θ ($\theta \in [0, \pi]$), which is the angle between two successive segments, $P_n P_{n+1}$ and $P_{n+1} P_{n+2}$, the path following performance will be degraded, because it is difficult to change the vessel heading in time. If R_0 is too large with large θ , the vessel trajectory will deviate from the current waypoint P_{n+1} significantly. Therefore, there exists a relationship between

the acceptance circle radius R_0 and path angle θ for good tracking performance, i.e., small deviations from the reference path.

In view of the deficiencies of a fixed acceptance circle radius, we propose an adaptive R_0 approach based on path angle θ considering the following conditions:

1. $R_{\min} \leq R_0 \leq R_{\max}$. R_{\min} should be set to avoid the radius of the acceptance circle too small; R_{\max} should be set such that the trajectory of the vessel around an waypoint does not deviate the reference path too much.
2. Analogous to the situation of driving a car, we need to turn earlier when driving a car to take a more sharper turn. When deciding the timing to switch to the next waypoint of ASVs, R_0 should have an inverse relationship with θ . Therefore, we can define $R_0 = \left(l\left(\frac{\pi}{\theta} - 1\right)^2 + M \right) L$ with $\frac{\pi}{\theta} - 1 \geq 0$, where M and l are unknown parameters with $l \geq 0$.

Based on the above conditions, R_0 is defined as

$$R_0 = \begin{cases} l\left(\frac{\pi}{\theta} - 1\right)^2 L + R_{\min}, & \forall \theta \geq \frac{\pi}{\sqrt{\frac{R_{\max}-R_{\min}}{l} + 1}} \\ R_{\max}, & \forall \theta < \frac{\pi}{\sqrt{\frac{R_{\max}-R_{\min}}{l} + 1}}, \end{cases} \quad (16)$$

where l is a positive scaling factors to be tuned and l should be chosen considering different manoeuvrability capabilities of different vessels. The steps for identifying l for a specific vessel are as follows:

1. Select n waypoints with different values of θ , i.e., $\{\theta_1, \theta_2, \dots, \theta_n\}$.
2. Test the performance of path following with a series of fixed acceptance circle radii. An evaluation index e_a , i.e., average cross error, for path following performance is defined as

$$e_a = \frac{1}{N_{\text{sim}}} \sum_{i=1}^{N_{\text{sim}}} |e(i)|, \quad (17)$$

where N_{sim} is the total number of steps during the simulation experiment, and $e(i)$ is the cross error e at time i . The smaller e_a is, the better the performance will be.

3. Find the optimal R_0 for each specific waypoint θ with (17), and the optimal sequence of R_0 is denoted by $\{\bar{R}_{01}, \bar{R}_{02}, \dots, \bar{R}_{0n}\}$. Theoretically, the larger n is, the more precise the estimator \hat{l} of l is. Usually, $n \geq 3$ is selected.
4. Apply the linear least square method to identify the value of l , and \hat{l} is calculated as follows:

$$\hat{l} = (\theta^T \theta)^{-1} \theta^T y, \quad (18)$$

where

$$\theta = \left[\left(\frac{\pi}{\theta_1} - 1\right)^2 \left(\frac{\pi}{\theta_2} - 1\right)^2 \dots \left(\frac{\pi}{\theta_n} - 1\right)^2 \right]^T, \\ y = \left[\frac{\bar{R}_{01} - R_{\min}}{L} \quad \frac{\bar{R}_{02} - R_{\min}}{L} \quad \dots \quad \frac{\bar{R}_{0n} - R_{\min}}{L} \right]^T.$$

In Sect. 4, we further illustrate this procedure in simulation experiments.

3.2 Nonlinear MPC-based path following controller with adaptive LOS

MPC methods utilize a system model for trajectory prediction and optimization. We take (5) as the system model. Considering that path following aims at making the cross error e , the ship relative heading $\tilde{\psi}$ and the rudder angle δ all converge to 0, the state-space equation (5) is transformed with defining a new state vector $\mathbf{x}_N = [x_{N1} \ x_{N2} \ x_{N3} \ x_{N4} \ x_{N5}]^T = [e \ \tilde{\psi} \ r \ \dot{r} \ \delta]^T$ based on (10) and (11) to

$$\dot{\mathbf{x}}_N(t) = f_N(\mathbf{x}_N(t), u(t)) + \mathbf{E}_N \mathbf{w}_N(t), \quad (19)$$

where $f_N(\mathbf{x}_N(t), u(t))$ is as follows:

$$f_N(\mathbf{x}_N, u) = \begin{bmatrix} u_0 \sin(x_{N2}) \\ x_{N3} \\ x_{N4} \\ g_2(\mathbf{x}_N, u) \\ \frac{1}{T_C} (K_C u - x_{N5}) \end{bmatrix}, \quad (20)$$

where $g_2(\mathbf{x}_N, u) = \frac{1}{T_1 T_2} \left[K x_{N5} + \frac{K T_3}{T_C} (K_C u - x_{N5}) - (T_1 + T_2) x_{N4} - x_{N3} - \alpha x_{N3}^3 \right]$, $\mathbf{E}_N \in \mathbb{R}^{5 \times 5}$, $\mathbf{w}_N \in \mathbb{R}^{5 \times 1}$.

For numerical simulations and implementation in practical applications, continuous time model (20) needs to be discretized. The commonly used Runge–Kutta method is selected for discretization. This method uses the formula:

$$\mathbf{x}_N(k+1) = \mathbf{x}_N(k) + \frac{T_s}{6} (d_1 + 2d_2 + 2d_3 + d_4), \quad (21)$$

where $d_1 = f_N(\mathbf{x}_N(k), u(k))$, $d_2 = f_N(\mathbf{x}_N(k) + \frac{T_s}{2} d_1, u(k))$, $d_3 = f_N(\mathbf{x}_N(k) + \frac{T_s}{2} d_2, u(k))$, $d_4 = f_N(\mathbf{x}_N(k) + T_s d_3, u(k))$. Equation (21) advances a solution from $\mathbf{x}_N(k)$ to $\mathbf{x}_N(k+1)$ with the time interval T_s . Considering that the control objective of path following is to minimize the cross error and energy consumption, the error between the state vector $\mathbf{x}_N = [e \ \tilde{\psi} \ r \ \dot{r} \ \delta]^T$ and the reference state vector $\mathbf{x}_{Nr} = [0 \ \tilde{\psi}_{\text{LOS}} \ 0 \ 0 \ 0]^T$ is minimized. Therefore, at each control time k , the following quadratic cost function $J(k)$ is minimized:

$$J(k) = \sum_{i=1}^{N_p} \mathbf{x}_{Ne}(k+i)^T \mathbf{Q} \mathbf{x}_{Ne}(k+i) + \sum_{i=1}^{N_c} u(k+i-1)^T \mathbf{R} u(k+i-1), \tag{22}$$

where $\mathbf{x}_{Ne}(k+i) = \mathbf{x}_N(k+i) - \mathbf{x}_{Nr}(k+i)$, where $\mathbf{x}_{Nr}(k+i)$ is the reference state vector at time $k+i$; N_p stands for the length of the prediction horizon; \mathbf{Q} and \mathbf{R} are weighting matrices. Meanwhile, considering the limitations of the actuator, input constraints should be satisfied during path following as

$$\delta_{\min} \leq u(k) \leq \delta_{\max}, \Delta\delta_{\min} \leq \Delta u(k) \leq \Delta\delta_{\max}, \tag{23}$$

where δ_{\min} , δ_{\max} , $\Delta\delta_{\min}$ and $\Delta\delta_{\max}$ are the limit values. Moreover, the following constraints need to be satisfied:

$$u(k+i-1) = u(k+N_c-1), N_c < i \leq N_p, \tag{24}$$

$$\mathbf{x}_N(k+i) = f(\mathbf{x}_N(k+i-1), u(k+i-1)), \tag{25}$$

where N_c stands for the length of the control horizon and satisfies $N_p \geq N_c$.

Therefore, at time k ($k \geq 1$), we solve the optimization problem:

$$\begin{aligned} \Delta u^*(k) &= \underset{\Delta u}{\operatorname{argmin}} J(k), \\ \text{subject to} & \\ (23), & \\ (24), & \\ (25). & \end{aligned} \tag{26}$$

Problem (26) is a nonlinear programming problem since $J(k)$ and (25) are nonlinear. The optimized control sequence is obtained at time k by solving (26) and the first element of time k optimized control sequence is set as system input at time k .

The predictive path following control algorithm is as follows:

1. Initialize the path parameters, i.e., the waypoints and the adaptive R_0 sequence with identified l , and the state $\mathbf{x}_N(k)$ ($k = 0$).
2. Solve (26) and obtain the optimized control sequence at time k ($k = 0, 1, 2, \dots$) $\mathbf{u}^*(k) = \{u^*(k), u^*(k+1), \dots, u^*(k+N_p-1)\}$.
3. Apply the control signal, i.e., the first element $u^*(k)$, to the system.

4. Acquire the real-time state $\mathbf{x}_N(k)$ by the perception system at time k if the vessel arrives at the destination, the sailing of the vessel stops; otherwise, go back to step 2, set $k = k + 1$, and continue.

4 Simulation experiments

In this section, we carry out simulation experiments involving a small-scale model ship in our laboratory. The model parameters of the model ship required for setting up model equation (4) have been identified with a least square identification method based on experimental data in a ship towing tank. The main geometric parameters of the model ship are shown in Table 2. The identified parameters in (4) with the surge speed $u_0 = 0.8$ m/s are: $K_C = 1.0000$, $K = 0.5060 \text{ s}^{-1}$, $T_1 = 1.2481 \text{ s}$, $T_2 = 0.1245 \text{ s}$, $T_3 = -0.0757 \text{ s}$, $\alpha = 0.0081 \text{ s}^2$, and $T_C = 0.1000 \text{ s}$.

The simulation and controller parameters are set as follows: discretization time span $T_s = 0.5 \text{ s}$, MPC prediction horizon length $N_p = 10$, control horizon length $N_c = 8$, the rudder magnitude constraint at time k : $-30^\circ \leq \delta(k) \leq 30^\circ$, the rudder rate constraint at time k : $-120^\circ T_s \leq \Delta\delta(k) \leq 120^\circ T_s$ ($\Delta\delta(k) = \delta(k) - \delta(k-1)$), $-120^\circ/\text{s} \leq \dot{\delta} \leq 120^\circ/\text{s}$, and the weight matrices \mathbf{Q} and \mathbf{R} are set to

$$\mathbf{Q} = \begin{bmatrix} 1 & 0 & 0 & 0 & 0 \\ 0 & 1 & 0 & 0 & 0 \\ 0 & 0 & 0.01 & 0 & 0 \\ 0 & 0 & 0 & 0.01 & 0 \\ 0 & 0 & 0 & 0 & 0.001 \end{bmatrix}, \quad \mathbf{R} = 0.1.$$

Note that the weight matrices \mathbf{Q} and \mathbf{R} are chosen according to the control targets, i.e., the heading ψ and the error e have a more important impact on the path following performance in comparison of other states or input.

4.1 Identifying l for adaptive LOS guidance

We first investigate the effect of the size of the acceptance circle on the path following performance. Considering that the tracking path should have different path angles θ to verify

Table 2 Model ship main parameters

Item	Notation	Value	Unit
Length	L	0.95	m
Breadth	B	0.24	m
Mass	m	5.40	kg
Nominal speed	U	0.8	m/s

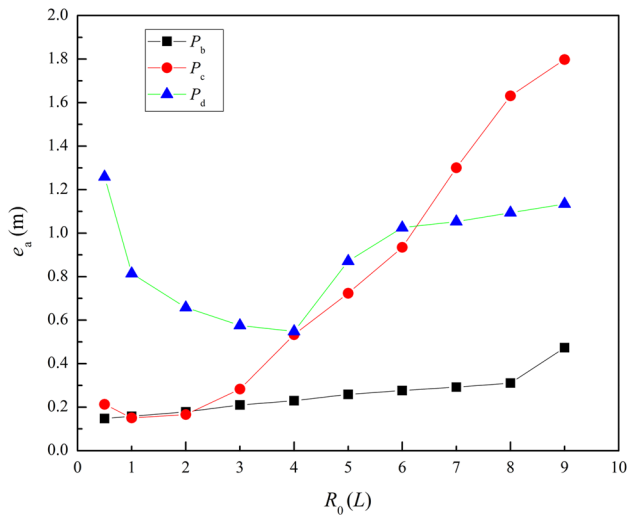


Fig. 4 Average cross errors comparison with different acceptance circle radii

the effectiveness of the proposed method, waypoints of a path named *Path 1* are set to: $P_a(1, 1)$, $P_b(11, 10)$, $P_c(20, 22)$, $P_d(40, 15)$ and $P_e(34, 1)$ in sequence, as shown in Fig. 5; the starting position and heading are set to $P_0(2, 1)$ and 45° , respectively. R_{min} and R_{max} are set to $0.5L$ and $9L$, respectively.

Figure 4 shows the performance of path following with different values of R_0 around the waypoints P_b , P_c , P_d and different acceptance circle radii, ranging from $0.5L$ to $9L$ evaluated. Figure 4 shows that there exists a different optimal R_0 radius to generate the least e around an relevant waypoint because of a different angle of the waypoint.

Using the data from Fig. 4, we can identify l in (16). The optimal radii of different angles θ_b , θ_c , and θ_d are $\bar{R}_{0b} = 0.5L$, $\bar{R}_{0c} = 1L$, and $\bar{R}_{0d} = 4L$, respectively. We obtain $\hat{l}_1 = 2.7$ with (18). To verify the effectiveness of (18) for different paths with the identified l , a different path, i.e., *Path 2* in Fig. 6, is defined as: $P'_a(1, 1)$, $P'_b(15, 1)$, $P'_c(25, 7)$, $P'_d(25, 25)$, $P'_e(45, 25)$; the starting position and heading are set to $P_0(1, 2)$ and 90° , respectively. With the identified l , the R_0 radius sequences of *Path 1* and *Path 2* are $S_1 = \{0.5L, 1.8L, 3.7L\}$ and $S_2 = \{0.6L, 1.1L, 3.2L\}$, respectively.

4.2 Path following control with adaptive LOS and MPC

To verify the effectiveness of adaptive LOS guidance with variable acceptance circle radius, the performance of the

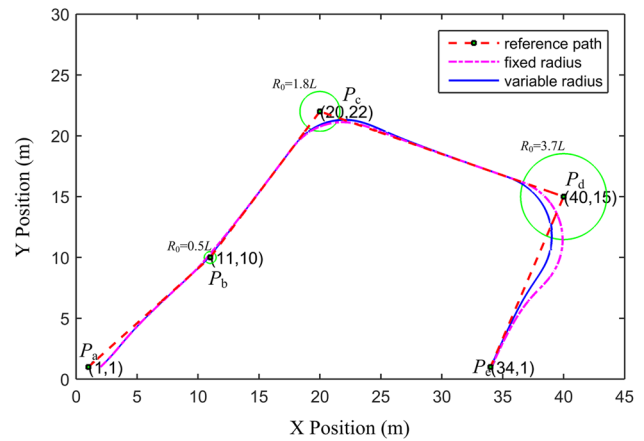


Fig. 5 Obtained trajectories with *Path 1*, $R_0 = 2L$, and variable R_0

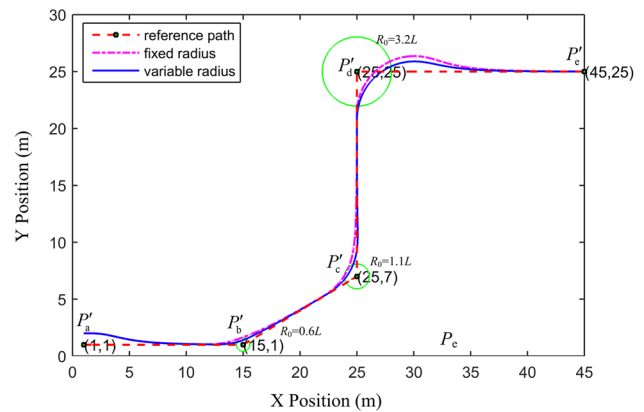


Fig. 6 Obtained trajectories with *Path 2*, $R_0 = 2L$, and variable R_0

entire *Path 1* and *Path 2* with different fixed and variable R_0 is compared in Table 3, where e_{a1} and e_{a2} are the evaluation index of *Path 1* and *Path 2*, respectively. e_a with variable R_0 , i.e., S_1 and S_2 , in both *Path 1* and *Path 2* are the minimum, and smaller than the minimum among all the fixed R_0 . The trajectories obtained for the scenarios with *Path 1* and *Path 2* with variable R_0 and $R_0 = 2L$ that has the best performance among fixed acceptance circle radii are given in Figs. 5 and 6. The trajectory with adaptive LOS guidance is closer to the reference path both in *Path 1* and *Path 2*. The errors e with adaptive LOS guidance are compared in Fig. 7 with the fixed $R_0 = 2L$ in *Path 1* and *Path 2*.

Table 3 Performance under different fixed and variable R_0

$R_0(L)$	Fixed									Variable	
	0.5	1.0	2.0	3.0	4.0	5.0	6.0	7.0	8.0		9.0
$e_{a1}(m)$	0.67	0.42	0.33	0.34	0.43	0.59	0.78	1.00	1.27	1.57	0.29
$e_{a2}(m)$	0.53	0.36	0.35	0.41	0.47	0.67	0.89	1.11	1.38	1.68	0.28

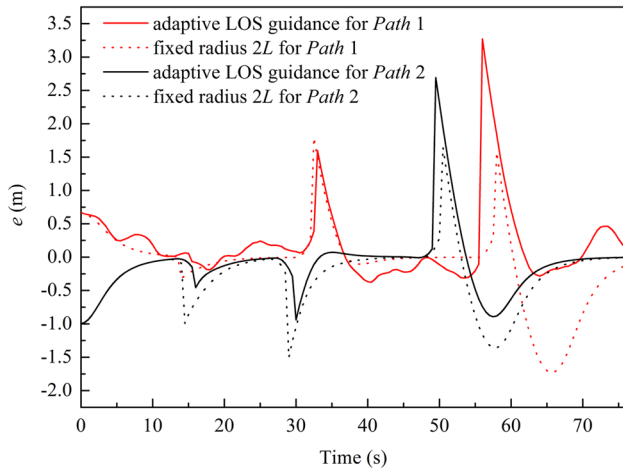


Fig. 7 Errors e with adaptive LOS guidance and fixed $R_0 = 2L$ in Path 1 and Path 2

4.3 Influences of disturbances

The ability to resist disturbances for a path following controller is essential to guarantee a good performance and vessel safety. For this reason, it is necessary to compare the performance obtained with disturbances and without disturbances. In the simulation, the conditions of disturbances are as follows:

$$\mathbf{E}_N = \begin{bmatrix} 0.15 & 0 & 0 & 0 & 0 \\ 0 & 1.50 & 0 & 0 & 0 \\ 0 & 0 & 1.50 & 0 & 0 \\ 0 & 0 & 0 & 1.50 & 0 \\ 0 & 0 & 0 & 0 & 1.50 \end{bmatrix},$$

$$\mathbf{w}_N(t) = [\tau_1, \tau_2, \tau_3, \tau_4, \tau_5],$$

where $\tau_1 \sim \tau_5 \in [-1, 1]$ are random disturbances with normal distribution. Note that the first element of the main diagonal of \mathbf{E}_N , i.e., $(\mathbf{E}_N)_{11} = 0.15$, is different from other elements of the main diagonal, i.e., $(\mathbf{E}_N)_{22}$, $(\mathbf{E}_N)_{33}$, $(\mathbf{E}_N)_{44}$ and $(\mathbf{E}_N)_{55}$, because $(\mathbf{E}_N)_{11}$ stands for the disturbance weight for cross error e , but $(\mathbf{E}_N)_{22}$, $(\mathbf{E}_N)_{33}$, $(\mathbf{E}_N)_{44}$ and $(\mathbf{E}_N)_{55}$ stand for the disturbance weights for measurement errors, i.e., $\tilde{\psi}$, r , \dot{r} and δ , respectively. Actually, the weight matrix \mathbf{E}_N can also be changed on the basis of a specific disturbance environment. Using the adaptive LOS guidance with variable acceptance circle radii, the trajectories obtained under path following without disturbances and with disturbances are shown in Fig. 8.

The input rudder angle δ , cross error e , and heading ψ are shown in Figs. 9, 10, and 11, respectively. The input rudder angle with disturbances varies more rapidly

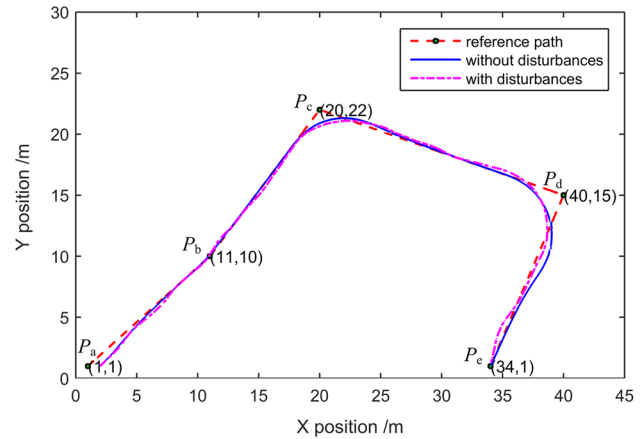


Fig. 8 Trajectories of the model ship with disturbances and without disturbances

than without disturbances, because the rudder should be manipulated more frequently to counteract the effects of disturbances. The vessel with disturbances can also track the path and its error is not significantly different from the error without disturbances. Moreover, it is possible that the tracking errors with disturbances are sometimes smaller than the errors without disturbance, because the disturbances change the vessel heading randomly. However, when the disturbances is larger than the limitation for the control system, it is not able to control the trajectory to track the reference path any more. In Fig. 11, the heading without disturbances turns to be stabilized gradually during tracking the straight path while the heading with disturbances fluctuate within a limited range.

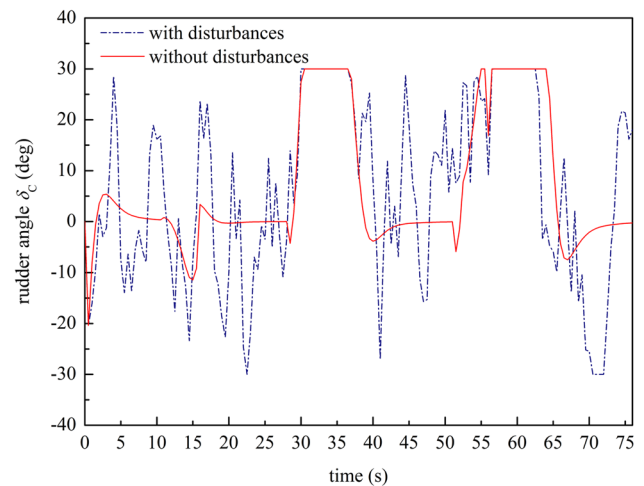


Fig. 9 Input rudder angle with disturbances and without disturbances

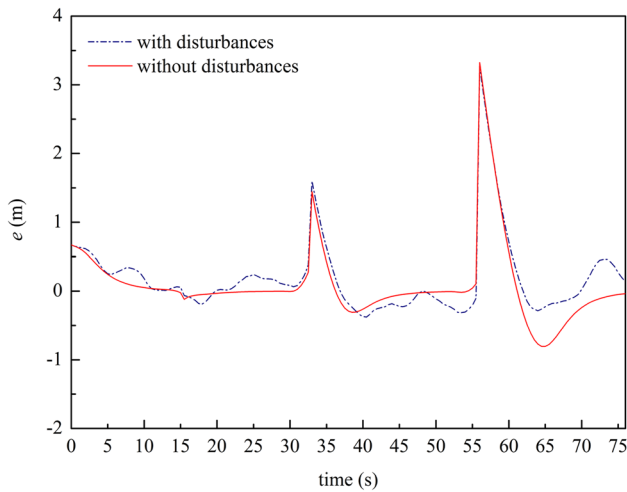


Fig. 10 Error with disturbances and without disturbances

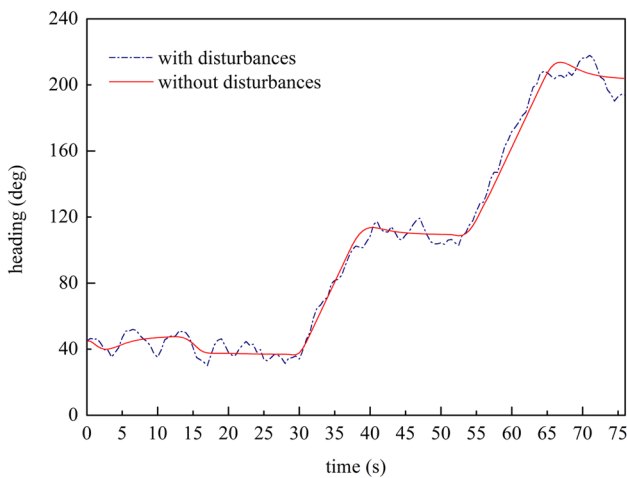


Fig. 11 Heading with disturbances and without disturbances

5 Conclusions and future research

This paper investigates the problems of finding the most suitable model for underactuated ASVs and more accurate LOS guidance for path following. Models for path following are reviewed and concluded according to different categories. The difficulties of parameter identification of different models are analyzed. Then, the second-order Nomoto nonlinear model is proposed for a path following controller design for ASVs. Compared with other nonlinear models, it is more convenient to identify the parameters of this model. Moreover, an LOS guidance algorithm with variable acceptance circle sizes is proposed. Results obtained with simulation experiments illustrate that a variable acceptance circle size can be effective with respect to reducing cross-tracking errors in path following. The path following

method based on the above model, the proposed LOS guidance, and an MPC algorithm is elaborated on and verified by the simulation experiments without disturbances and with disturbances. Considering that the proof of MPC stability is usually based on assumptions that the control horizon length is infinite or there exist strict terminal state constraints [39], most of these assumptions are not realistic for a practical application. Hence, the stability of the proposed controller in this paper is not discussed, instead, we verify the proposed control method with plenty of simulation scenarios.

Further research will extend the numerical simulations to a real vessel platform and solve the real time and robust optimization problems during practical applications. Moreover, adaptive identification of model parameters in different vessel sailing conditions will be considered.

Acknowledgements This research is supported by the China Scholarship Council under Grant 201506950053, the National Natural Science Foundation of China (NSFC) Project (Project 61273234), the Natural Science Foundation of Hubei Province Project (Project 2015CFA111), and the Project of Ministry of Transport, China (Project 2015326548030).

References

1. Yan R, Pang S, Sun H, Pang Y (2010) Development and missions of unmanned surface vehicle. *J Mar Sci Appl* 9(4):451–457
2. Do KD, Jiang ZP, Pan J (2004) Robust adaptive path following of underactuated ships. *Automatica* 40(6):929–944
3. Zhao J, Tan M, Price WG, Wilson PA (1994) DCPA simulation model for automatic collision avoidance decision making systems using fuzzy sets. In: *Proceedings of the oceans 94, IEEE, Brest, France, vol 2, pp 244–249*
4. Zhao J, Price WG, Wilson PA, Tan M (1995) The uncertainty and uncoordination of mariners’ behaviour in collision avoidance at sea. *J Navig* 48(03):425–435
5. Li Z, Sun J, Oh SR (2009c) Design, analysis and experimental validation of a robust nonlinear path following controller for marine surface vessels. *Automatica* 45(7):1649–1658
6. Moreira L, Fossen TI, Soares CG (2007) Path following control system for a tanker ship model. *Ocean Eng* 34(14):2074–2085
7. Fossen TI (2011) *Handbook of marine craft hydrodynamics and motion control*. Wiley, West Sussex
8. Oh SR, Sun J (2010) Path following of underactuated marine surface vessels using line-of-sight based model predictive control. *Ocean Eng* 37(2):289–295
9. Liu C, Sun J, Zou Z (2015a) Integrated line of sight and model predictive control for path following and roll motion control using rudder. *J Ship Res* 59(2):99–112
10. Skjetne R, Jørgensen U, Teel AR (2011) Line-of-sight path-following along regularly parametrized curves solved as a generic maneuvering problem. In: *Proceedings of the 2011 IEEE conference on decision and control and European control conference, Orlando, USA, pp 2467–2474*
11. McGooin EW, Murray-Smith DJ, Li Y, Fossen TI (2000) Ship steering control system optimisation using genetic algorithms. *Control Eng Pract* 8(4):429–443
12. Fossen TI, Breivik M, Skjetne R (2003) Line-of-sight path following of underactuated marine craft. In: *Proceedings of the 6th*

- IFAC manoeuvring and control of marine craft, Girona, Spain, pp 244–249
13. Wilson PA, Harris CJ, Hong X (2003) A line of sight counteraction navigation algorithm for ship encounter collision avoidance. *J Navig* 56(01):111–121
 14. Do KD, Pan J (2006) Underactuated ships follow smooth paths with integral actions and without velocity measurements for feedback: theory and experiments. *IEEE Trans Control Syst Technol* 14(2):308–322
 15. Mcgookin EW, Murray-Smith DJ, Li Y, Fossen TI (2000) Experimental results from supply ship autopilot optimization using genetic algorithms. *J Inst Meas Control* 22(2):141–178
 16. Zheng H, Negenborn RR, Lodewijks G (2016) Predictive path following with arrival time awareness for waterborne AGVs. *Transp Res Part C Emerg Technol* 70:214–237
 17. Tzeng C, Chen J (1999) Fundamental properties of linear ship steering dynamic models. *J Mar Sci Technol* 7(2):79–88
 18. Witkowska A, Tomera M, Śmierczalski R (2007) A backstepping approach to ship course control. *Int J Appl Math Comput Sci* 17(1):73–85
 19. Fossen TI, Lauvdal T (1994) Nonlinear stability analysis of ship autopilots in sway, roll and yaw. In: *Proceedings of the 3rd conference on marine craft maneuvering and control (MCMC'94)*, Southampton, UK, pp 113–124
 20. Li Z, Sun J, Oh S (2009b) Path following for marine surface vessels with rudder and roll constraints: an MPC approach. In: *Proceedings of the 2009 American control conference*, St. Louis, USA, pp 3611–3616
 21. Y KYP, Lefeber E (2001) Way-point tracking control of ships. In: *Proceedings of the 40th IEEE conference on decision and control*, IEEE, Orlando, USA, vol 1, pp 940–945
 22. Caharija W, Pettersen KY, Sørensen AJ, Candeloro M, Gravdahl JT (2014) Relative velocity control and integral line of sight for path following of autonomous surface vessels: merging intuition with theory. *Proc Inst Mech Eng Part M J Eng Marit Environ* 228(2):180–191
 23. Daly JM, Tribou MJ, Waslander SL (2012) A nonlinear path following controller for an underactuated unmanned surface vessel. In: *Proceedings of the 2012 intelligent robots and systems conference*, Vilamoura, Portugal, pp 82–87
 24. Moe S, Caharija W, Pettersen KY, Schjølberg I (2014) Path following of underactuated marine surface vessels in the presence of unknown ocean currents. In: *Proceedings of the 2014 American control conference*, Portland, USA, pp 3856–3861
 25. Breivik M, Fossen TI (2004) Path following for marine surface vessels. In: *Proceedings of the 2004 TECHNO-OCEAN conference*, Kobe, Japan, vol 4, pp 2282–2289
 26. Do K (2015) Global path-following control of underactuated ships under deterministic and stochastic sea loads. *Robotica* 34(11):2566–2591
 27. Liu C, Zou Z, Yin J (2014) Path following and stabilization of underactuated surface vessels based on adaptive hierarchical sliding mode. *Int J Innov Comput Inf Control* 10:909–918
 28. Liu C, Zou Z, Li T (2015b) Path following of underactuated surface vessels with fin roll reduction based on neural network and hierarchical sliding mode technique. *Neural Comput Appl* 26(7):1–11
 29. Zhang G, Zhang X, Zheng Y (2015) Adaptive neural path-following control for underactuated ships in fields of marine practice. *Ocean Eng* 104:558–567
 30. Li T, Yu B, Hong B (2009a) A novel adaptive fuzzy design for path following for underactuated ships with actuator dynamics. In: *Proceedings of the 2009 industrial electronics and applications*, Xi'an, China, pp 2796–2800
 31. Oh SR, Sun J, Li Z, Celkis EA, Parsons D (2010) System identification of a model ship using a mechatronic system. *IEEE Trans Mechatron* 15(2):316–320
 32. Caharija W, Pettersen KY, Gravdahl JT (2013) Path following of marine surface vessels with saturated transverse actuators. In: *Proceedings of the 2013 American control conference*, Washington, USA, pp 546–553
 33. Meng W, Guo C, Liu Y (2012) Robust adaptive path following for underactuated surface vessels with uncertain dynamics. *J Mar Sci Appl* 11(2):244–250
 34. Valenciaga F (2014) A second order sliding mode path following control for autonomous surface vessels. *Asian J Control* 16(5):1515–1521
 35. Pavlov A, Nordahl H, Breivik M (2009) MPC-based optimal path following for underactuated vessels. In: *Proceedings of the 8th IFAC international conference on manoeuvring and control of marine craft*, Guarujá, Brazil, pp 340–345
 36. Ghommam J, Mnif F, Benali A, Derbel N (2009) Nonsingular Serret–Frenet based path following control for an underactuated surface vessel. *J Dyn Syst Meas Control* 131(2):021006:1–021006:8
 37. Velagic J, Vukic Z, Omerdic E (2003) Adaptive fuzzy ship autopilot for track-keeping. *Control Eng Pract* 11(4):433–443
 38. Skjetne R, Fossen TI (2001) Nonlinear maneuvering and control of ships. In: *Proceedings of the 2001 MTS/IEEE oceans conference and exhibition*, Honolulu, USA, pp 1808–1815
 39. Mayne D, Rawlings J, Rao C, Scokaert P (2000) Constrained model predictive control: stability and optimality. *Automatica* 36(6):789–814